Human Activity Classification Based on MicroDoppler Signatures Using a Support Vector Machine

Youngwook Kim[1] and Hao Ling[2]

[1] Department of Electrical and Computer Engineering
California State University at Fresno

[2]Department of Electrical and Computer Engineering
University of Texas at Austin
Email: youngkim@csufresno.edu, ling@ece.utexas.edu

Abstract: The feasibility of classifying different human activities based on microDoppler signatures is investigated. Measured data of 12 human subjects performing seven different activities are collected using a Doppler radar. The seven activities include running, walking, walking while holding a stick, crawling, boxing while moving forward, boxing while standing in place, and sitting still. Six features are extracted from the Doppler spectrogram. A support vector machine (SVM) is then trained using the measurement features to classify the activities. The multi-class classification is implemented using a decision tree structure. Optimal parameters for the SVM are found through a four-fold cross validation. The resulting classification accuracy is found to be more than 90%. The potentials of classifying human activities over extended time duration, through wall, and at oblique angles with respect to the radar are also investigated and discussed.

Published in *IEEE Trans. Geosci. Remote Sensing*, 47: 1328-1337, May 2009.

Digital Object Identifier 10.1109/TGRS.2009.2012849

1. Introduction

Due to the increasing demand for physical security and surveillance, one of the emerging applications of radar recently is the detection and tracking of people in a highly cluttered environment [1-11]. For instance, it is desirable to locate humans through walls and extract information on their activities in real time by using electromagnetic based sensors. The applications of through-wall human monitoring include disaster search-and-rescue, physical security, law enforcement, and urban military operations.

There has been a significant amount of research for developing human detection and tracking sensors. One approach is the use of wide bandwidth to achieve high resolution imaging in the down-range dimension. Several studies have shown promising results from imaging building interiors to ultimately detecting and tracking humans in indoor environments as reported in [2-8]. Another choice is to use a Doppler radar [1, 9-22]. Doppler-based radars are excellent for detecting movement while suppressing any stationary clutters in the background. Low-cost sensors using off-the-shelf components or even single-chip modules are readily available. Finally, a very unique and interesting aspect of Doppler returns from humans is the appearance of "microDoppler" features [9, 12]. MicroDopplers are generated from the non-rigid-body motions of humans, and contain valuable information related to human movements. Since it was first reported in [9], a number of works have appeared on exploiting microDopplers for human classification. For example, van Dorp [13] estimated the parameters of human gait from FMCW radar data. Otero [14] designed a simple classifier to recognize walking humans using a spectral analysis. In [15-17], microDoppler features of radar target returns were extracted through various time-frequency analyses. MicroDoppler features were explored to distinguish among humans, animals and vehicles in [18-22]. In this

paper, we pose a different research question, namely, whether it is possible to distinguish various human activities such as walking, running, crawling, etc. based on the microDoppler features. The reliable recognition of simple human activities may be a first step toward addressing the more difficult yet important question of determining human intent.

Our approach is to apply a support vector machine (SVM), trained using measured microDoppler data, to classify activities of a human. SVM is a binary classifier that constructs a maximal-margin hyperplane to separate data between classes [23-25]. It has been used extensively for many diverse classification problems due to its superior performance over other classification methods such as the Fisher linear discriminator and the Bayesian decision method. In the radar community, SVM has been applied to array signal processing [26, 27] and radar target recognition [28, 29] problems. In this study, we consider 7 different human activities including running, walking, walking while holding a stick, crawling, boxing while moving forward, boxing while standing in place, and sitting still. In order to recognize the activities, the time-varying Doppler signatures are examined using the short-time Fourier transform and different features are extracted from the spectrogram. Based on the extracted features, an SVM is constructed to classify the seven activities. For the generation of training data, measurements on twelve human subjects are collected in the laboratory using a 2.4GHz Doppler radar [10]. To implement a multi-class problem using the SVM, which is a binary classifier, a decision-tree based structure is employed. The training process and the resulting classification accuracy are evaluated. The importance of each feature is also investigated. Finally, the potentials of classifying human activities over extended time duration, through wall, and at oblique angles with respect to the radar are investigated and discussed.

This paper is organized as follows. The measurement data collection of the different

human activities is described in Sec. 2. Sec. 3 discusses the feature selection and extraction process from the spectrogram. In Sec. 4, the concept and training results of the SVM are described. Sec. 5 addresses some additional issues of monitoring humans including through-wall. Sec. 6 presents the conclusion.

2. MEASUREMENT OF DIFFERENT HUMAN ACTIVITIES

Measured data of 12 human subjects undergoing different activities are collected using a Doppler radar testbed [10]. The radar operates at 2.4 GHz. The transmitter operates in the continuous wave mode. The receiver comprises a microstrip antenna connect to a commercial integrated receiver board. The antennas are installed to collect vertical polarization data. Since the human body is typically vertically elongated, the use of vertical polarization results in a stronger radar return. The received signals are down-converted and then digitized (at 1 kHz) for off-line processing. The measurements are performed in an indoor environment under the line-of-sight condition. Only a single human subject is tested at one time, with the subject moving directly toward the radar. The range of the measurement is between 2 m and 8 m.

Data for human subjects undergoing seven different activities are collected, including: (a) running, (b) walking, (c) walking while holding a stick (using both hands), (d) crawling, (e) boxing while moving forward, (f) boxing while standing in place, and (g) sitting still (with slight fidgeting movements). An illustration of the performed activities is shown in Fig. 1. The descriptions of each activity are given in Table 1. The data are collected over a six second interval. The short-time Fourier transform (STFT) is then applied to the data to generate the

corresponding spectrogram. A 0.25-second Kaiser window is used in the STFT. The resulting spectrograms of the seven activities from one particular subject are shown in Fig. 2.

Table 1. Seven human activities under study.

Activity	Description
(a). Running	The act of running forward quickly by moving arms and legs.
(b). Walking	The act of walking forward at a moderate speed while moving arms and legs.
(c). Walking while holding a stick	The act of walking while holding a wooden stick in a horizontal position using both hands.
(d). Crawling	The act of crawling on both hands and knees while moving forward on the ground.
(e). Boxing while moving forward	The act of throwing punches using both arms while walking forward.
(f). Boxing while standing in place	The act of throwing punches using both arms while standing still.
(g). Sitting still	The act of sitting in a chair with slight fidgeting movements such as shaking of legs, touching of hair, or crossing of arms.

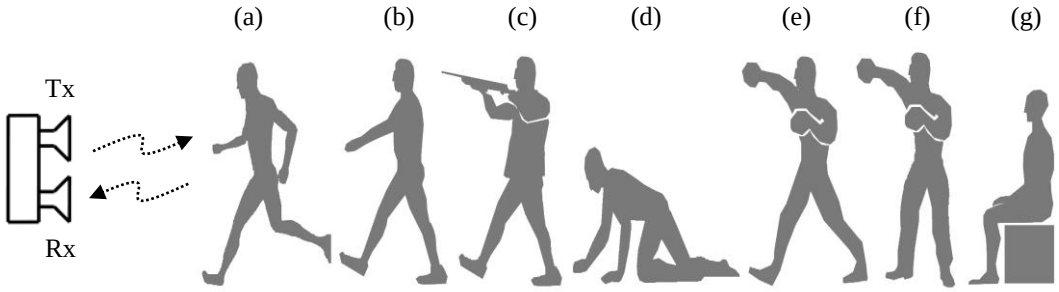

Fig. 1. Illustration of measurements of seven different human activities.

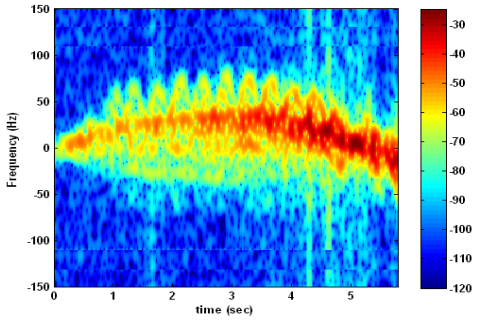

(a) Running

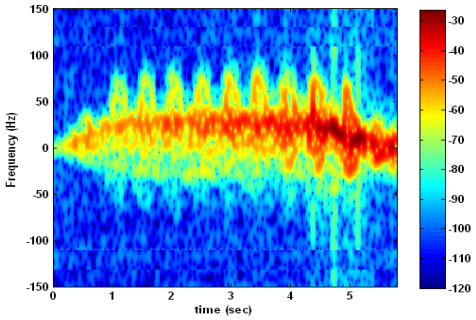

(b) Walking

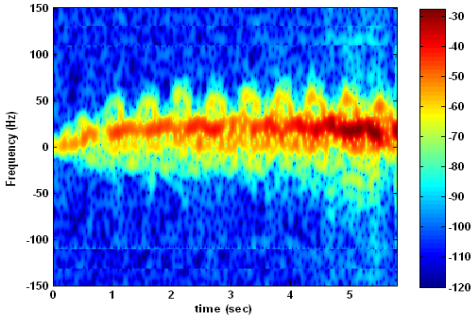

(c) Walking while holding a stick

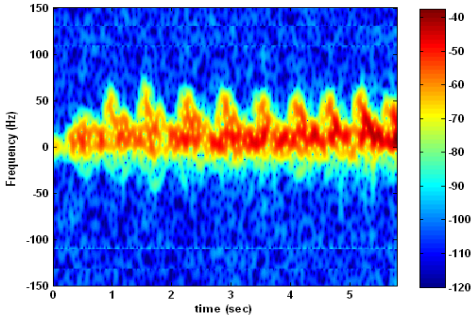

(d) Crawling

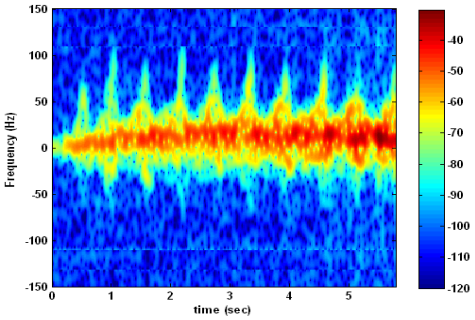

(e) Boxing while moving forward

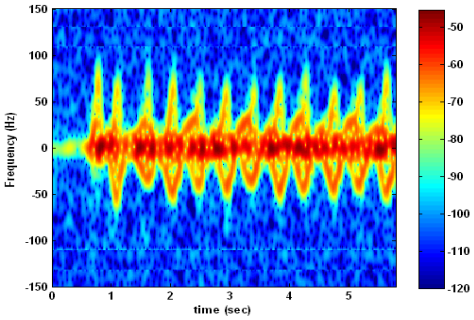

(f) Boxing while standing in place

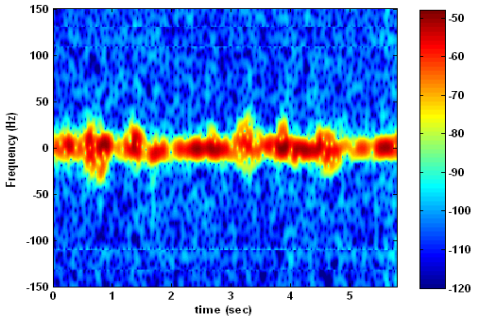

(g) Sitting with slight movements

Fig. 2. Spectrograms of seven human activities.

As seen in Fig. 2, the spectrograms show rather interesting and distinct signatures depending on the activity. The strongest return in each spectrogram comes from that of the torso, while the periodic microDoppler modulations surrounding the torso return come from arm and leg movements. Among all the activities, the running motion has the highest Doppler frequency due to the torso, which can be as high as 30 Hz. It also has a wide Doppler signal spread, which can be as large as 120 Hz. The walking motion shows similar Doppler patterns with the running case, except the maximum Doppler shift from the torso is lower (20 Hz) and the period of the microDoppler is longer. Walking while holding a stick has a similar spectrogram with the walking case, but it has a slightly narrower microDoppler frequency spread. In the crawling motion, the torso Doppler is nearly zero. In addition, the spectrogram shows that most of the microDopplers are skewed toward the positive with respect to the torso Doppler. This is expected since contrary to the earlier motions, there is no back-swing in the crawling motion. In the boxing while standing in place motion in Fig. 2(f), periodic microDopplers from the arms are clearly observed. In Fig. 2(e), the boxing while moving forward motion has a positive torso Doppler component in addition to the

microDopplers from the arms. In comparison to normal walking, it is also clear that the microDoppler spread is quite wide due to the rapid punching motion. The sitting still has almost a zero torso frequency and shows small, sporadic microDopplers due to fidgeting motions. These characteristics of Doppler signatures will be extracted in the next section.

3. Feature Extraction and Training Data Generation

3.1. Doppler Signal Detection and Feature Extraction. In order to extract distinct Doppler features from a spectrogram, it is necessary to distinguish the Doppler signal from noise. A key issue is the determination of a noise threshold. A histogram of the signal strength of the noise (i.e., received signal with no target present) is shown in Fig. 3(a). In the figure, the noise is found to have a Gaussian-like distribution. Fig. 3(b) shows a histogram when the human Doppler signal is present. Thus the lowest power level at which the signal histogram starts to deviate from the Gaussian-like noise distribution can be used as the noise threshold, which, reading from the figure, is −83 dBm. Using this threshold, the spectrogram of a representative activity (boxing while standing in place) is processed and shown in Fig. 4. We note here that while this approach works well in the present line-of-sight situation, it may not work in more complex environments containing interference, through-wall or multi-path effects.

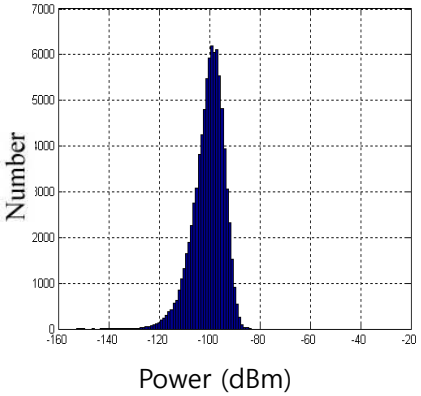

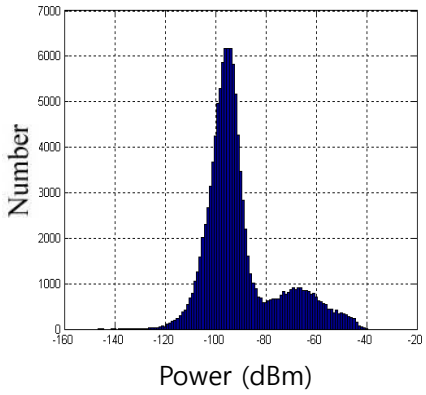

(a) (b)

Fig. 3. (a) Histogram of the noise, (b) Histogram of the target return and noise.

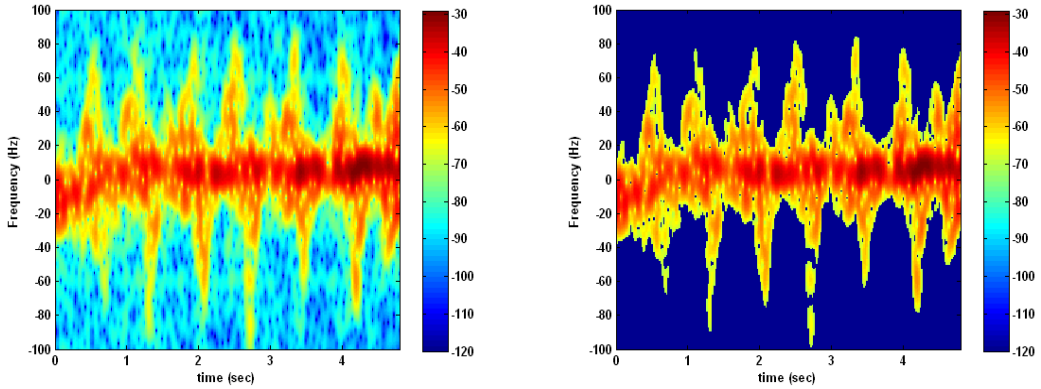

(a) (b)

Fig. 4: Spectrogram of the boxing while standing in place motion. (a) Before the processing, (b) After thresholding.

Next, different Doppler features are extracted from the de-noised spectrogram. The spectrogram itself can be used as input to a classifier without any processing to identify different activities. However, such high dimensional data would result in a classifier with a very complex inner structure and thus an enormous training process. The proper choice of features can reduce data dimensions while maintaining the essential characteristics of the microDoppler signatures. Based on the initial observations in Sec. 2, we choose the following six features to characterize the microDoppler signatures: (1) the torso Doppler frequency, (2) the total bandwidth (BW) of the Doppler signal, (3) the offset of the total Doppler, (4) the bandwidth without microDopplers, (5) the normalized standard deviation (STD) of the Doppler

signal strength, and (6) the period of the limb motion. An illustration of the features is depicted in Fig. 5.

The torso Doppler frequency (1) corresponds to the speed of the human subject. The human torso speed is a very basic yet important piece of information since there is a large variation in the torso speed depending on the different activities. The total bandwidth of the Doppler signal (2) is related to the speed of the limb motions. A large bandwidth results from fast swings of arms or legs. The offset of the total Doppler signal (3) is a measure of the asymmetry between the forward and backward motions of the limbs. This offset would be the same as the torso speed if the forward and backward swings are exactly symmetrical when the limbs move back and forth. The bandwidth without microDopplers (4) represents the Doppler bandwidth of the torso alone. It accounts for the bobbing motion of the torso while the human performs an activity. The normalized STD of the Doppler signal strength (5) is related to the dynamic range of the motion. For example, a large motion like running tends to have a high standard deviation in the Doppler signal strength, while sitting still has a small value. We normalize the STD value by the mean of the Doppler signal strength to eliminate the effect of distance between the human subject and the radar. The period of the limb motion (6) corresponds to the swing rate of the arms and legs.

A Matlab routine is written to extract these six features automatically by processing data over a three-second time window. The torso Doppler frequency (1) is the average frequency of the peak signal in strength over the time bins within the window. For the calculation of features (2), (3), (4) and (6), two signal envelopes are first identified. The highest Doppler frequency at each time bin makes up a high-frequency envelope. The lowest Doppler frequency at each time bin makes up a low-frequency envelope. The bandwidth (2) is the

averaged difference between the largest frequencies from the high frequency envelope and the smallest frequencies from the low frequency envelope. The offset of the Doppler frequency (3) is the mean value between the largest frequencies of the high-frequency envelope and the smallest frequencies of the low-frequency envelope. The bandwidth without microDopplers (4) is the averaged difference between the smallest frequencies from the high-frequency envelope and the largest frequencies from the low-frequency envelope. Feature (5) is the standard deviation of the signal strength divided by the average of the signal strength of all the above-noise Doppler signals in the spectrogram. The period (6) is the time period of the microDoppler from the limbs.

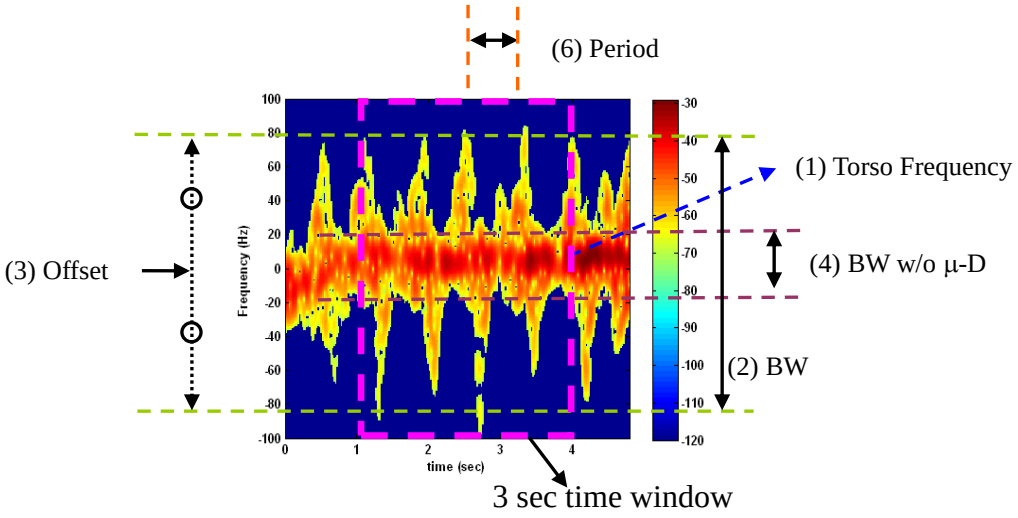

Fig. 5. Selected features of the Doppler spectrogram.

3.2. Training Feature Set Generation. A classifier implemented using a machine learning technique requires a training data set. In our study, the data set is constructed by extracting the

features from the measured data, which consists of 12 human subjects performing seven activities. Each human subject repeats a particular activity for six seconds four different times. Then we use a three-second time window to extract three different realizations of the features per measurement. Thus, 12 realizations of each activity from a particular person are formed. The total number of feature sets is (12 subjects) x (7 activities) x (12 realizations) = 1008.

The mean values of each feature from all 12 subjects are shown in Table 2. It can be seen that the mean values show clear differences among activities, making classification potentially possible. However, by also examining the histograms (not shown here), we find that the distributions show considerable overlap with one another. This means it is not an easy task to construct a classifier to distinguish the activities, and a more sophisticated classifier like the SVM is therefore needed.

Table 2. Mean values of the six features.

	Feature 1	Feature 2	Feature 3	Feature 4	Feature 5	Feature 6
Activity (a)	29.209	128.654	20.127	104.50	1.772	0.425
Activity (b)	22.430	120.159	21.157	85.341	1.725	0.528
Activity (c)	19.430	100.352	19.717	69.093	1.378	0.520
Activity (d)	6.491	63.691	13.570	39.197	1.294	0.539
Activity (e)	11.101	89.205	17.365	60.402	1.432	0.474
Activity (f)	0.172	97.537	5.679	50.119	0.918	0.424
Activity (g)	-0.055	30.862	-0.041	23.384	0.851	0.529

4. HUMAN ACTIVITY CLASSIFICATION USING SVM

An SVM is applied to classify the seven human activities based on the features extracted from the Doppler spectrogram. SVM is a binary classifier developed by Vapnik [23-25]. It is a supervised learning method that is based on a kernel technique. The original optimal hyperplane algorithm is limited to a linear classification problem. However, SVM is developed to create a nonlinear class boundary by applying the kernel technique to achieve the maximum margin between classes. Through the kernel technique, the input data are transformed to a high dimensional space. In the transformed feature space, the data may be classified by a linear hyperplane. The linear optimal hyperplane results in a nonlinear boundary in the original input space. Because the classification accuracy depends on the kernel used, the selection of kernel is very critical in practice.

We utilize *LibSVM*, a freely available SVM library implemented by Chang and Lin [30]. For the given penalty parameter and the kernel parameter, *LibSVM* constructs the decision boundary based on the training data and then calculates the classification error for the validation data. In our case, three quarters of the data collected are used for the training data set, and the remaining one quarter is used as the validation set.

For the training procedure, two scenarios are used as shown in Fig. 6. The first scenario uses all the data from nine subjects for training and the data from the remaining three subjects for validation. The second scenario uses nine realizations of all twelve subjects as the training set, and the remaining three realizations of all the subjects as the validation set. The first scenario is more realistic because it classifies the activities of unknown humans based on the data from known subjects. The second scenario classifies a person's activity based on training data that include that individual. The final classification error is calculated using a

four-fold cross validation. In the validation, the error is calculated four times with different combinations of training and validation data set for the given total data set. This process generalizes the performance of the SVM and is summarized in Fig. 7. Successful training should result in both small average error and small error variance.

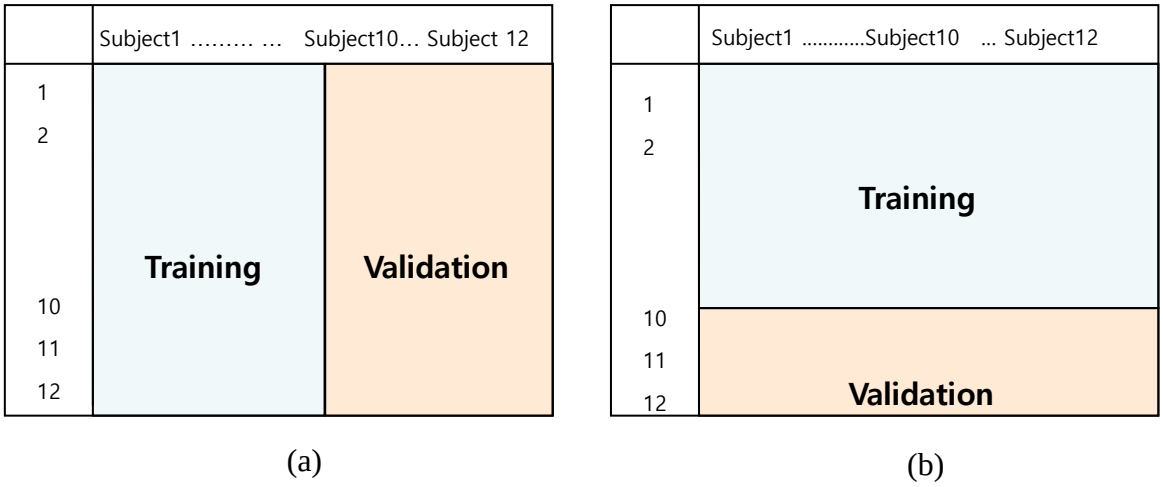

Fig. 6. Training and validation data set for the four-fold validation. (a) The first scenario. (b) The second scenario.

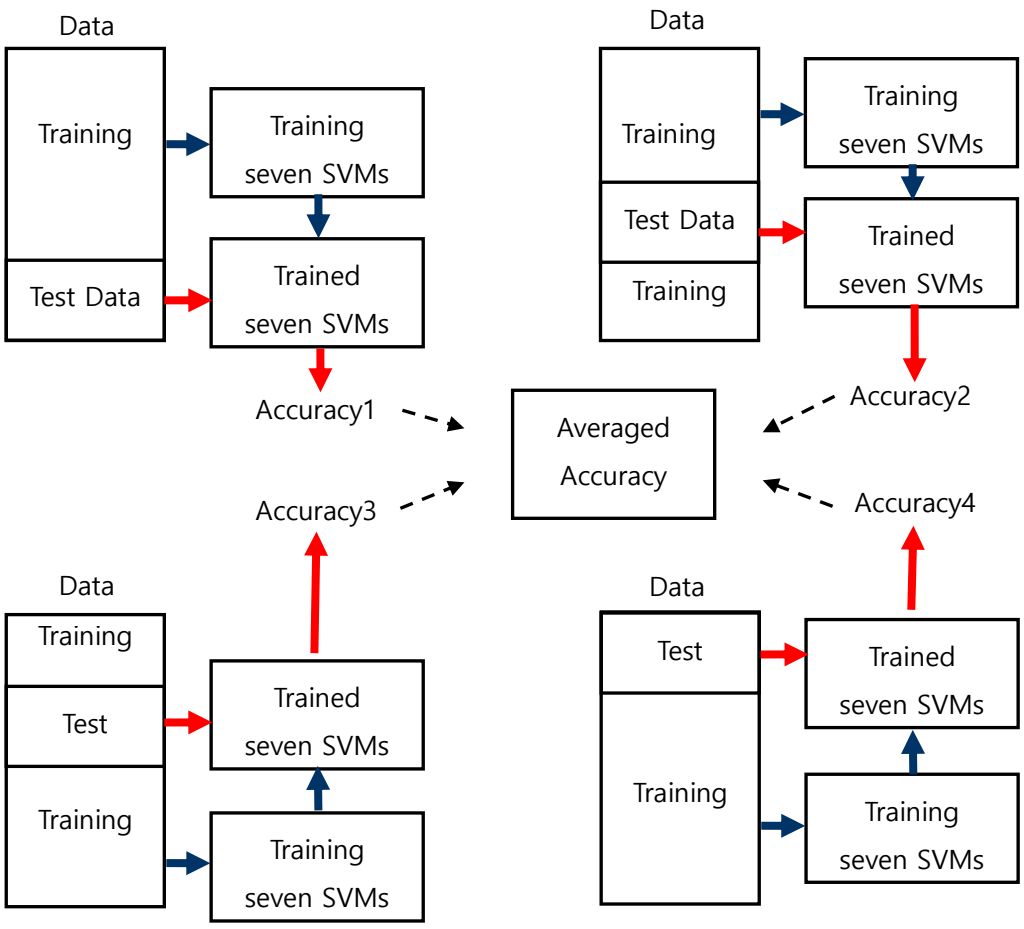

Fig. 7. The process of four-fold validation.

The formulation of the SVM is based on the two-class problem. In order to apply an SVM to the multi-class problem like the one at hand, it should be reformulated into several binary class problems. Different methods have been developed to handle such multi-class problems using SVMs [31, 32]. In this paper, we apply SVMs to a decision tree classifier. The decision tree method breaks multiple classes into several distinct binary decision problems using a tree structure. At each non-leaf node of the structure, a binary SVM classifier is used. A decision-tree based SVM is selected because it is simple and intuitive. Furthermore, it requires

the least number of SVMs to be trained and has the shortest training and testing time. The configuration of the suggested decision tree is shown in Fig. 8. Six different SVMs should be constructed. Each SVM uses a different amount of training data. For example, the training data set for SVM1 consists of activities (a),(b),(c),(d),(e),(f) and (g). That of SVM3 is from only activities (b) and (c).

In our decision tree struture, SVM1 is used at the top node to separate all activities into two groups: a group with high torso speed and a group with low torso speed. Among the group with high torso speed, the running activity (a) is separated from other two through SVM2, while SVM3 is used to classify between activities (b) and (c). SVM4, SVM5 and SVM6 are used to divide the group with low torso speed into specific activities. We note that this structure is constructed heuristically so that it may not be optimal.

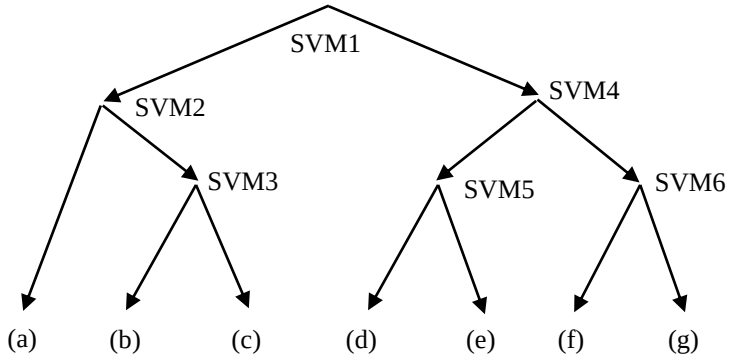

Fig. 8. Suggested decision tree using SVM.

We use the Gaussian kernel for the construction of the SVMs. For successful learning, the penalty parameter of the SVM and the Gaussian kernel width should be carefully

determined. The optimal values are searched exhaustively to have the minimum average classification error over the four-fold cross validation for each SVM.

For the first scenario, the average and the variance of the validation error of classification are 0.081 and 0.007, respectively. For the second scenario, the average and the variance of the validation error of classification are 0.072 and 0.010. The second scenario has slightly smaller validation error, or better accuracy (92.8% vs. 91.9%), as compared to that of the first case. This is expected since the second scenario classifies a person's activity based on training data that include that individual. It is also worth noting that the performance of the SVM is better than that of an artificial neural network classifier [33], which achieved a classification accuracy in the mid-80 percent range.

The resulting averaged confusion matrices are shown in Table 3. The boxing while moving forward (e) has the highest classification error in the first scenario, but it has a very small error in the second scenario. We believe this is caused by the large deviations in how each subject performs this activity. Thus, predicting an unknown person's activity results in a high error. We also observe that the walking while holding a stick (c) activity is easily confused with the walking (b) activity in both scenarios. This shows that such a fine motion difference is harder to detect. In particular, at 2.4 GHz, the Doppler resolution is poor and the arm microDoppler is very much buried inside the microDoppler from the leg motions. The only distinction between the two activities appears to be the slightly smaller average values of all six features in activity (c) in comparison to activity (b), as shown earlier in Table 2.

Table 3. Results of the SVM based on a decision tree structure. (a) Confusion matrix for the first scenario. (b) Confusion matrix for the second scenario. *Es* represents the estimated class, and *Ac* represents the actual class. The number represents the percentage of correct classification in each case.

(a) (b)

Es\Ac	(a)	(b)	(c)	(d)	(e)	(f)	(g)
(a)	97	0	0	0	0	0	0
(b)	0	82	17	0	2	0	0
(c)	3	18	81	0	4	0	0
(d)	0	0	0	95	6	0	0
(e)	0	0	2	5	78	1	0
(f)	0	0	0	0	10	99	0
(g)	0	0	0	0	0	0	100

Es\Ac	(a)	(b)	(c)	(d)	(e)	(f)	(g)
(a)	95	0	0	0	0	0	0
(b)	1	83	15	0	0	0	0
(c)	2	17	85	0	3	0	0
(d)	0	0	0	89	1	0	0
(e)	0	0	0	11	96	0	0
(f)	2	0	0	0	0	100	0
(g)	0	0	0	0	0	0	100

The SVM classification of activities using the Doppler features results in a low validation error. However, it is instructive to investigate which features are more important in the classification. First, we carry out the classification process using one single feature at a time. The four-fold validation error trained with only a given feature is shown in Table 4. From the table, the orders of features in terms of classification performance are as follows: the torso frequency (feature 1), the BW without microDopplers (4), the total BW (2), the offset of the total Doppler (3), the normalized STD (5), and the period (6). The torso frequency alone can achieve a 70% performance, while the classification accuracies from the normalized STD of signal strengths and the period are only around 30%.

Table 4. Classification error only with a particular feature.

Particular Feature	(1)	(2)	(3)	(4)	(5)	(6)
Error (Accuracy)	0.299 (70.1%)	0.456 (54.4%)	0.552 (44.8%)	0.350 (65.0%)	0.682 (31.8%)	0.697 (30.3%)

Next, we evaluate the combined effect of these features by adding the features one at a time based on the orders determined above. Note that since the features can interact in a complex way in the classification process, it is not easy to predict the exact effect of combining features. The classification accuracy as more features are added sequentially is depicted in Fig. 9. As expected, more features result in a higher accuracy overall. However, the last two features, namely, the normalized STD of signal strengths and the period only improve the result very marginally. Therefore, good accuracy can be achieved with only the four most important features.

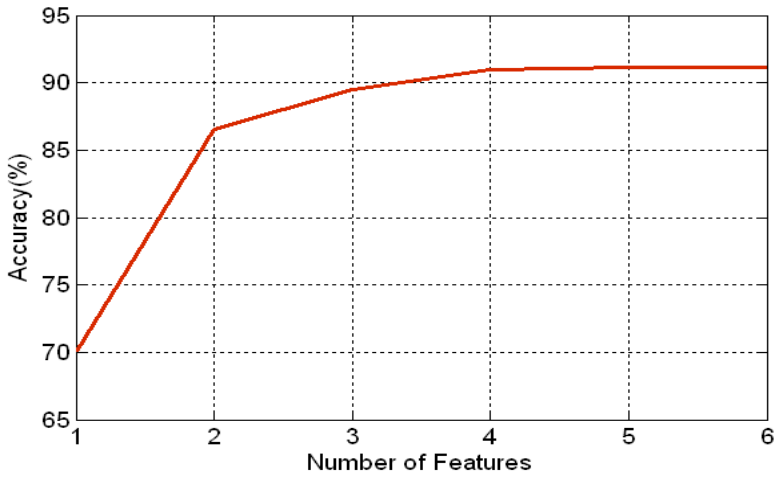

Fig. 9. Accuracy of the SVM classification with an increasing of number of input features.

5. ADDITIONAL INVESTIGATIONS

5.1. Classification of a Sequence of Activities. In practice, human behaviors may consist of a sequence of activities when observed over an extended time period, transitioning from one activity to another. It would be useful to investigate whether it is possible to reliably classify human activities on a continuous basis. If so, then it may be possible to determine higher-order human intent through the classification of a series of simple activities discussed previously. With the SVM classifier we have developed for single-event activities, one question is how it will perform during the transition between activities. Measurement data from a person undergoing a sequence of activities over a longer time duration are collected and tested using the constructed SVM. A three-second time window is first applied to the data and input to the classifier. The window is then slid forward by 0.5 second at a time and the process is repeated onward. Two cases are considered for the sequential activities. The first case comprises crawling motion (d), followed by boxing while standing in place (f), followed by walking (b). The second case comprises walking (b), boxing while standing in place (f), and boxing while moving forward (e), followed by walking while holding a stick (c). Figs. 10(a) and (b) present the measured spectrograms and the classification results for the two cases. The SVM predicts the activities of the first case correctly except for the transition from boxing while standing in place to walking. The misclassification region is shaded in the figure. In the transition, the activity is classified as boxing while moving forward (e). Because the features are averaged values in the three-second time window, the classification can be erroneous when the activity changes during the time window. However, the misclassified result of boxing while moving forward (e) is not unreasonable as it can be regarded as a combination of boxing while standing in place (f) and walking (b). The second case has two intervals where

misclassifications occur. The transition from walking (b) to boxing while standing in place (f) is again misclassified as boxing while moving forward (e) by the SVM. The transition from boxing moving forward (e) to walking while holding a stick (c) is classified as sitting still (g). Since these transitional motions are not included in the training data, the results for these intervals can be interpreted as examples of how our classifier performs under an unknown activity. With its structure, the classifier simply forces a decision based on the match in the extracted features.

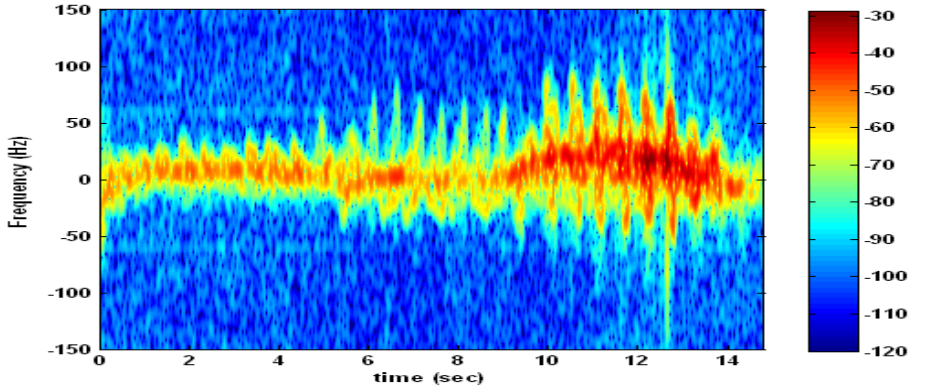

(a)

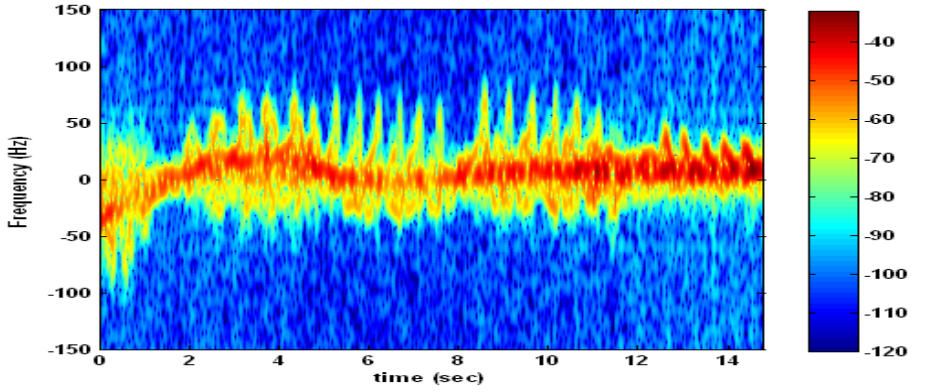

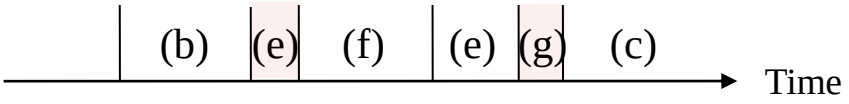

(b)

Fig. 10. Spectrograms of a sequence of activities and their classification results, (a) Crawling, boxing while standing in place, followed by walking, (b) Walking, boxing while standing in place, boxing while moving forward, followed by walking while holding a stick.

5.2. Oblique Angle Case. In the collected data, the human subject always moves directly toward the radar. This will not in general be true in a more realistic situation. To assess the effect of the oblique angle case, the seven activities of a particular human subject are measured when the subject approaches to the radar while maintaining a 30 degree angle with respect to the radial direction. The measurement setup and the path are shown in Fig. 11(a). Note that to maintain a fixed 30 degree angle with respect the radial direction, the chosen path is not straight. The subject repeats the seven activities four times. Features from 12 realizations are extracted in the same manner as before for each activity. The previously trained SVM based on the head-on data under the second scenario is then used to classify to the newly measured data. The result shows almost the same classification performance. The classification accuracy was 91.4% (vs. 92.8%). It is believed that the accuracy is not significantly deteriorated because the effect of the oblique-angle case is just a scaling of the Doppler information and the amount is not large when the angle is not too large. Fig. 11(b) shows a spectrogram from the walking

case. Very little difference exists between this figure and the head-on walking data shown in Fig. 2(b).

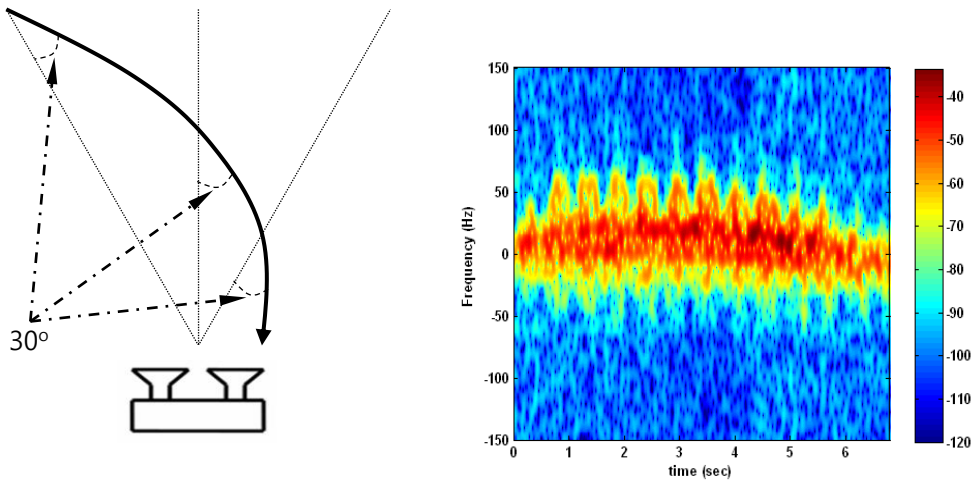

(a) (b)

Fig. 11. (a) The trajectory of the oblique angle (30-degree) case, (b) Measured spectrogram for the walking motion.

5.3. Through-wall Measurements: In-situ through-wall measurements are also performed to see how the microDoppler features are affected by wall. The test is carried out on an exterior building wall, which is a 40-cm thick brick wall. The radar is placed in the interior of the building 0.1 m behind the wall, and a human subject carries out the activities on the other side of wall outside the building. The signal experiences approximately a 25 dB two-way attenuation due to the wall. Moreover, the noise level is increased by 11 dB due to the reflection of the incident signal from the wall. Thus, the signal-to-noise ratio (SNR) suffers a

36 dB reduction. The histograms of noise signal strength for the line-of-sight and through-wall cases are shown in Fig. 12. It would be much more difficult to detect the target from noise due to the reduced SNR.

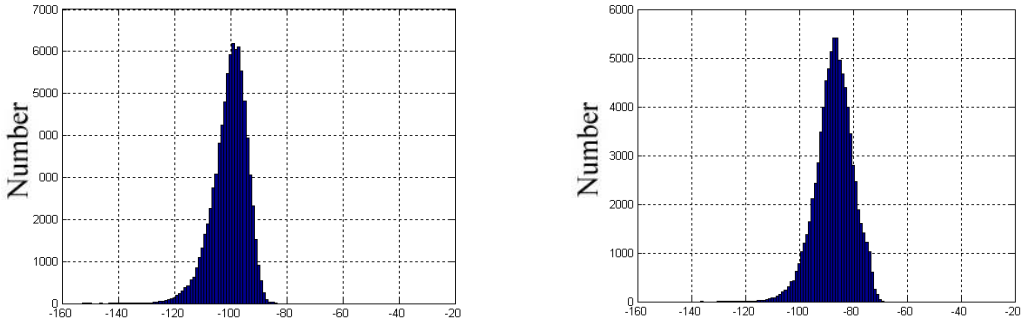

(a) (b)

Fig. 12. (a) Histogram of noise in case of line-of-sight, (b) Histogram of the through-wall case.

Fig. 13 shows the spectrograms of the walking and the crawling activity measured in the through-wall environment. The 60Hz AC line can now be seen due to the much lower signal level. The human subject approaches the radar as time progresses. While the torso return can be still seen, it is now much more difficult to identify the microDopplers when the human subject is far from the radar (more than 4 m). When the human is within 4 m from the wall, the microDoppler signatures of each activity can be better observed, although the limited SNR is still troublesome for our current feature extractor. While this through-wall result is somewhat pessimistic, we believe the main bottleneck is in our radar hardware. With a pulsed waveform and more sophisticated timing to avoid transmitter jamming, a significant

improvement in the SNR may be possible. Other than the SNR issue, our recent study has shown that the wall effect on the Doppler frequency is actually quite negligible [30].

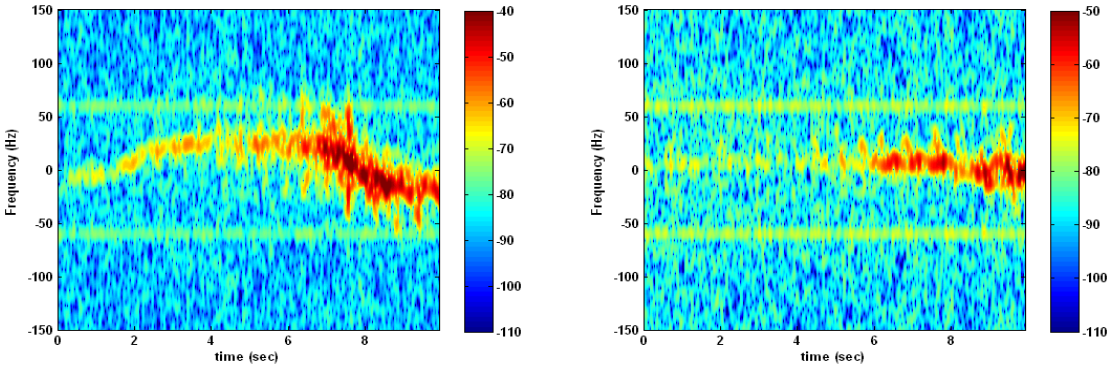

(a) (b)

Fig. 13. (a) Through-wall measurement of the walking activity, (b) Through-wall measurement of the crawling activity.

6. CONCLUSION

In this paper, we investigated the feasibility of classifying different human activities based on microDoppler signatures. Measured data of 12 human subjects performing seven different activities were collected using a Doppler radar. Six features were extracted from the Doppler spectrogram. An SVM was then trained using the measurement features to classify the activities. The multi-class classification was implemented using a decision tree structure. The classification accuracy based on the six features was found to be above 90%.

While the results shown in the this paper are promising, we also briefly investigated the possibility of classifying human activities over an extended time duration, at oblique angles

with respect to the radar and through a wall. Among the three issues, through-wall human classification remains the most challenging problem. The low SNR in our measurements made the use of microDoppler signatures very difficult. Improved hardware is needed to overcome the transmitter jamming issue. Additional studies of the wall phenomenology are also needed to understand the effect of different walls on the microDoppler features.

We found that a 30-degree oblique approach angle with respect to the radar did not significantly impact the classification results. However, more severe degradation may occur at larger angles. It may be necessary to consider distributed Doppler sensors to classify the activities of human moving in any direction.

Finally, the classification of a sequence of human activities when observed over an extended period of time was investigated. Using a moving window approach, we were able to use the developed classifier to successfully classify activities on a continuous basis. This approach may be a good first step toward determining the intent of a human by a sequence of basic activities.

Acknowledgments

This work was supported by the National Science Foundation under grant CBET-0730924 and the A.D. Hutchison Fellowship from the University of Texas at Austin.

References

[1] L. M. Frazier, “Motion detector radar for law enforcement,” *IEEE Potentials*, vol. 16, pp. 23 - 26, Jan. 1998.

[2] S. Nag, M.A. Barnes, T. Payment and G. Holladay, "Ultrawideband through-wall radar for detecting the motion of people in real time," *SPIE Proc. Radar Sensor Technology and Data Visualization*, vol. 4744, pp.48-57, July 2002.

[3] G. Franceschetti, J. Tatoian, D. Giri and G. Gibbs, "Timed arrays and their application to impulse SAR for through-the-wall imaging," *IEEE Antennas Propagat. Soc. Int. Symp. Digest,* vol. 3, pp. 3067 – 3070, June 2004.

[4] A. R. Hunt, "A wideband imaging radar for through-the-wall surveillance," *SPIE Proc.*, *Sensors, and Command, Control, Communications, and Intelligence (C3I) Technologies*, vol. 5403, pp. 590 – 596, Sept. 2004.

[5] L. Song, C. Yu and Q. Liu, "Through-wall imaging (TWI) by radar: 2-D tomographic results and analyses," *IEEE Trans. Geos. Remote Sensing*, vol. 43, pp. 2793 - 2798, Dec. 2005.

[6] Y. Yang and A. E. Fathy, "See-through-wall imaging using ultra-wideband short-pulse radar system*," IEEE Antennas Propagat. Soc. Int. Symp. Digest*, vol. 3B, pp. 334 – 337, July 2005.

[7] R. Solimene, R. Soldovieri and G. Prisco "A multiarray tomographic approach for through-wall imaging," *IEEE Trans. Geos. Remote Sensing*, vol. 46, pp. 1192 - 1199, April. 2008.

[8] M. Dehmollaian and K. Sarabandi, "Refocusing through building walls using synthetic aperture radar," *IEEE Trans. Geos. Remote Sensing*, vol. 46, pp. 1589 - 1599, June 2008.

[9] J. L. Geisheimer, E. F. Greneker and W. S. Marshall, "High-resolution Doppler model of the human gait," *SPIE Proc. Radar Sensor Technology and Data Visualization*, vol. 4744, pp. 8-18, July 2002.

[10] A. Lin and H. Ling, "A Doppler and direction-of-arrival (DDOA) radar for multiple-mover sensing based on a two-element array," *IEEE Trans. Aerosp. Electron. Syst.*, vol. 43, pp. 1496 – 1509, Oct. 2007.

[11] P. Setlur, M. Amin, F. Ahmad and T. Thayaparan, "Indoor imaging of targets enduring simple harmonic motion using Doppler radars," *IEEE Int. Symp. Signal Proc. Info. Tech*., pp. 141-146, Dec. 2005.

[12] V. C. Chen and H. Ling, *Time Frequency Transforms for Radar Imaging and Signal Analysis*, Artech House, Boston, MA, 2002.

[13] P. van Dorp and F.C.A. Groen, "Human walking estimation with radar," *IEE Proc. Radar Sonar Navig*., vol. 150, pp. 356-365, Oct. 2003.

[14] M. Otero, "Application of a continuous wave radar for human gait recognition," *SPIE Proc. Signal Processing, Sensor Fusion, and Target Recognition*, vol. 5809, pp. 538-548, May 2005.

[15] J. Li and H. Ling, "ISAR feature extraction from non-rigid body targets using adaptive chirplet signal representation," *IEE Proc. Radar Sonar Navig.*, vol. 150, pp. 284-291, Aug. 2003.

[16] T. Thayaparan, S. Abrol, E. Riseborough, L. Stankovic, D. Lamothe, and G. Duff, "Analysis of radar micro-Doppler signatures from experimental helicopter and human data," *IET Radar Sonar Navig*., vol. 1, pp. 289-299, Aug. 2007.

[17] P. Setlur, M. Amin and F. Ahmad, "Urban target classifications using time-frequency micro-Doppler signatures," *9th Int. Symp. Signal Proc. Its App.*, pp. 1-4, Feb. 2007.

[18] A.G. Stove and S.R. Sykes, "A Doppler-based automatic target classifier for a battlefield surveillance radar," *IEEE Radar Conf*., pp. 419-423, Oct. 2002.

[19] I. Bilik, J. Tabrikian and A. Cohen, "GMM-based target classification for ground surveillance Doppler radar," *IEEE Trans. Aerospace Electron. Syst*., vol. 42, pp. 267-278, Jan 2006.

[20] G. E. Smith, K. Woodbridge and C. J. Baker, "Template based micro-Doppler signature classification," *European Radar Conf.*, pp. 158-161, Sept. 2006.

[21] M. Anderson and R. Rogers, "Micro-Doppler analysis of multiple frequency continuous wave radar signatures," *SPIE Proc. Radar Sensor Technology*, vol. 6547, May 2007.

[22] G. E. Smith, K. Woodbridge and C. J. Baker, "Naïve Bayesian radar micro-doppler recognition," *Int. Conf. Radar*, pp. 111-116, Sept. 2008.

[23] V. Vapnik, *Statistical Learning Theory*, New York, Wiley, 1998.

[24] N. Cristianini and J. Shawe-Taylor, *An Introduction to Support Vector Machines and Other Kernel-based Learning Methods*, Cambridge University Press, 2000.

[25] T. Hastie, R. Tibshirani and J. Friedman, *The Elements of Statistical Learning*, Springer, 2001.

[26] M.M. Ramon, X. Nan and C.G. Christodoulou, "Beamforming using support vector machines," *IEEE Antennas Wireless Propagat. Lett*., vol. 4, pp. 439 – 442, 2005.

[27] M.M. Ramon, J.L. Rojo-Alvarez, G. Camps-Valls and C.G. Christodoulou, "Kernel antenna array processing," *IEEE Trans. Antennas Propagat*., vol. 55, pp. 642-650, Mar. 2007.

[28] Q. Zhao and J.C. Principe, "Support vector machine for SAR automatic target recognition," *IEEE Trans. Aerosp. Electron. Syst*., vol. 37, pp. 643-654, April 2001.

[29] B. Krishnapuram, J. Sichina and L. Carin, "Physics-based detection of targets in SAR imagery using support vector machines," *IEEE Sensors J.*, vol. 3, pp. 147-157, April 2003.

[30] C. Chang and C. Lin, *LIBSVM : a library for support vector machines*, 2001. Software available at http://www.csie.ntu.edu.tw/~cjlin/libsvm

[31] T. Fumitake and A. Shigeo, "Decision-tree-based multi-class support vector machines," *IEEE Proc. of ICONIP'02*, vol. 3, pp. 1418-1422, 2002.

[32] C. Hsu and C. Lin, "A comparison of methods for multiclass support vector machines," *IEEE Trans. Neural Networks*, vol. 13, pp. 415-425, Mar. 2002.

[33] Y. Kim and H. Ling, "Human activity classification based on micro-Doppler signatures using an artificial neural network," *IEEE Antennas Propagat. Soc. Int. Symp. Digest*, pp. 1-4, San Diego, CA, July 2008.

[34] Y. Kim, "Through-wall human monitoring using data-driven models with Doppler information," PhD Dissertation, The University of Texas at Austin, May 2008.